

**$O(\alpha_s v^2)$  corrections to hadronic and electromagnetic decays of  $^1S_0$  heavy quarkonium**

Huai-Ke Guo\* and Yan-Qing Ma†

*Department of Physics and State Key Laboratory of Nuclear Physics and Technology, Peking University, Beijing 100871, China*

Kuang-Ta Chao‡

*Department of Physics and State Key Laboratory of Nuclear Physics and Technology,  
and Center for High Energy Physics, Peking University, Beijing 100871, China*

(Received 15 April 2011; published 21 June 2011)

We study  $O(\alpha_s v^2)$  corrections to decays of  $^1S_0$  heavy quarkonium into light hadrons and two photons within the framework of nonrelativistic QCD and find these  $O(\alpha_s v^2)$  corrections to have significant contributions especially for the decay into light hadrons. With these new results, experimental measurements of the hadronic width and the  $\gamma\gamma$  width of  $\eta_c$  can be described more consistently. By fitting experimental data, we find the long-distance matrix elements of  $\eta_c$  to be  $|\mathcal{R}_{\eta_c}(0)|^2 = 0.834^{+0.281}_{-0.197} \text{ GeV}^3$  and  $\langle v^2 \rangle_{\eta_c} = 0.232^{+0.121}_{-0.098}$ . Moreover,  $\eta_c(2S)$  is also discussed and the  $\gamma\gamma$  decay width is predicted to be  $3.34^{+2.06}_{-2.10} \text{ KeV}$ .

DOI: 10.1103/PhysRevD.83.114038

PACS numbers: 12.38.Bx, 13.20.Gd, 14.40.Pq

**I. INTRODUCTION**

Heavy quarkonium plays an important role in establishing and understanding quantum chromodynamics (QCD), the fundamental theory of strong interactions. Because of the existence of several energy scales involved with these systems, heavy quarkonium provides an ideal laboratory for testing the perturbative and nonperturbative effects of QCD. An effective theory suitable for describing these systems is nonrelativistic QCD (NRQCD) [1], which is derived from QCD by considering the underlying nonrelativistic properties. According to NRQCD factorization [2], decays of heavy quarkonium into light hadrons or photons can be organized in a hierarchy of long-distance matrix elements (LDMEs), which are classified in terms of  $v$ , the relative velocity of the heavy quarks in heavy quarkonium.

Decays of  $^1S_0$  heavy quarkonium into light hadrons (LH) and two photons are among the simplest processes. The short-distance coefficients for corresponding LDMEs at leading order in  $v$  have been computed previously to next-to-leading order (NLO) in  $\alpha_s$  [2–12]. Moreover, that coefficient for  $\gamma\gamma$  decay has been calculated to next-to-next-to-leading order (NNLO) in  $\alpha_s$  [13]. However, all coefficients of LDMEs beyond leading order in  $v$  are known at best to leading order in  $\alpha_s$  [6,14–16]. It is well known that the calculation at leading order in  $\alpha_s$  suffers from large uncertainties due to strong renormalization scale dependence. Therefore, to give a more precise description for  $^1S_0$  heavy quarkonium decays beyond leading order in  $v$ , QCD corrections to these coefficients are apparently needed.

In this paper, we will study QCD corrections to the coefficients of order  $v^2$  LDME, namely, corrections at

order  $\alpha_s v^2$  for  $^1S_0$  quarkonium decays. Up to this order of corrections, there are two unknown LDMEs which should be fixed. Unfortunately, lattice calculation of these LDMEs [17,18], though based on first principles, suffers from large uncertainties. In Refs. [19–21], a new method was introduced to estimate LDMEs by combining potential models, lattice calculation, and experimental data. This method will also be used in this paper to determine the two unknown LDMEs. Then with our calculated  $\alpha_s v^2$  corrections, we will be able to get updated estimates for the decay widths of  $^1S_0$  heavy quarkonium into light hadrons and two photons.

The rest of this paper is organized as follows. We briefly introduce the theoretical procedures for calculations of heavy quarkonium decays in Sec. II. In Sec. III, we describe kinematics and method of calculation for these processes. Results in perturbative QCD are summarized in Sec. IV, while corresponding results in perturbative NRQCD are summarized in Sec. V. By using the matching condition, we give the updated short-distance coefficients in Sec. VI to include our new  $\alpha_s v^2$  corrections. With these newly obtained results, we determine the two unknown LDMEs using potential models and make predictions for relevant decay widths in Sec. VII. Finally, in Sec. VIII, we present a brief summary.

**II. DECAY OF HEAVY QUARKONIUM IN NRQCD**

The Lagrangian of NRQCD is derived from the QCD Lagrangian by integrating out the degrees of freedom of order  $m_Q$ , the mass of the heavy quark. Local 4-fermion operators are added to accommodate the inclusive annihilation decay of heavy quarkonium which happens at scale of order  $m_Q$ . The Lagrangian of NRQCD is

$$\mathcal{L}_{\text{NRQCD}} = \mathcal{L}_{\text{light}} + \mathcal{L}_{\text{heavy}} + \delta\mathcal{L}. \quad (1)$$

\*huaike.guo@gmail.com

†yqma.cn@gmail.com

‡ktchao@th.phy.pku.edu.cn

Here  $\mathcal{L}_{\text{heavy}}$  describes nonrelativistic heavy quarks and antiquarks and is given by

$$\mathcal{L}_{\text{heavy}} = \psi^\dagger \left( iD_t + \frac{\mathbf{D}^2}{2m_Q} \right) \psi + \chi^\dagger \left( iD_t - \frac{\mathbf{D}^2}{2m_Q} \right) \chi, \quad (2)$$

where  $\psi$  is the Pauli spinor field that annihilates a heavy quark,  $\chi$  is the Pauli spinor field that creates a heavy antiquark, and  $D_t$  and  $\mathbf{D}$  are the time and space components of the gauge-covariant derivative  $D^\mu$ . Terms corresponding to light quarks and gluons are given by  $\mathcal{L}_{\text{light}}$  and

$$\mathcal{L}_{\text{light}} = -\frac{1}{2} \text{tr} G_{\mu\nu} G^{\mu\nu} + \sum \bar{q} i \not{D} q, \quad (3)$$

where  $G_{\mu\nu}$  is the gluon field strength tensor,  $q$  is the Dirac spinor field for light quarks, and the sum is over  $n_f$  flavors of light quarks. Relativistic corrections to the basic effective lagrangian  $\mathcal{L}_{\text{heavy}} + \mathcal{L}_{\text{light}}$  are included in  $\delta\mathcal{L}$  and its leading terms are those bilinear in the heavy quark or antiquark field,

$$\begin{aligned} \delta\mathcal{L}_{\text{bilinear}} = & \frac{c_1}{8m_Q^3} (\psi^\dagger (\mathbf{D}^2)^2 \psi - \chi^\dagger (\mathbf{D}^2)^2 \chi) \\ & + \frac{c_2}{8m_Q^2} (\psi^\dagger (\mathbf{D} \cdot \mathbf{g} \mathbf{E} - \mathbf{g} \mathbf{E} \cdot \mathbf{D}) \psi \\ & + \chi^\dagger (\mathbf{D} \cdot \mathbf{g} \mathbf{E} - \mathbf{g} \mathbf{E} \cdot \mathbf{D}) \chi) \\ & + \frac{c_3}{8m_Q^2} (\psi^\dagger (i\mathbf{D} \times \mathbf{g} \mathbf{E} - \mathbf{g} \mathbf{E} \times i\mathbf{D}) \cdot \boldsymbol{\sigma} \psi \\ & + \chi^\dagger (i\mathbf{D} \times \mathbf{g} \mathbf{E} - \mathbf{g} \mathbf{E} \times i\mathbf{D}) \cdot \boldsymbol{\sigma} \chi) \\ & + \frac{c_4}{2m_Q} (\psi^\dagger (\mathbf{g} \mathbf{B} \cdot \boldsymbol{\sigma}) \psi - \chi^\dagger (\mathbf{g} \mathbf{B} \cdot \boldsymbol{\sigma}) \chi), \end{aligned} \quad (4)$$

where  $E^i = G^{0i}$  and  $B^i = \frac{1}{2} \epsilon^{ijk} G^{jk}$  are the electric and magnetic components of the gluon field strength tensor  $G^{\mu\nu}$ .

Further corrections include the description of inclusive annihilation decay of heavy quarkonium and can be achieved by adding local 4-fermion interactions as

$$\delta\mathcal{L}_{4\text{-fermion}} = \sum_n \frac{f_n(\mu_\Lambda)}{m_Q^{d_n-4}} \mathcal{O}_n(\mu_\Lambda), \quad (5)$$

where  $\mu_\Lambda$  is the NRQCD factorization scale,  $\mathcal{O}_n(\mu_\Lambda)$  is the local 4-fermion operator,  $d_n$  is the naive scaling dimension of the operator, and  $f_n(\mu_\Lambda)$  is the short-distance coefficient which can be calculated perturbatively.

Thus the decay width of heavy quarkonium can be given by the following factorization formula

$$\Gamma(H) = \sum_n \frac{2 \text{Im} f_n(\mu_\Lambda)}{m_Q^{d_n-4}} \langle H | \mathcal{O}_n(\mu_\Lambda) | H \rangle, \quad (6)$$

where heavy quarkonium state in the Fock space can be written as [2]

$$\begin{aligned} |H^{(2S+1)L_J}\rangle = & O(1) |Q\bar{Q}^{(2S+1)L_J^{[1]}}\rangle \\ & + O(v) |Q\bar{Q}^{(2S+1)L \pm 1_J^{[8]}}g\rangle \\ & + O(v^2) |Q\bar{Q}^{(2S'+1)L_J^{[8]}}g\rangle \\ & + O(v^2) |Q\bar{Q}^{(2S+1)L_J^{[1,8]}}gg\rangle + \dots, \end{aligned} \quad (7)$$

and the relative importance of the 4-fermion operators regarding  $v$  can be accessed through the velocity scaling rules outlined in Ref. [2]. We conform to this standard NRQCD power counting rules throughout this work, although alternative power counting rules exist [22–24]. A detailed discussion of the influence of different power counting rules can be found in Ref. [20]. For  $^1S_0$  heavy quarkonium decays at order  $v^2$ , we need only consider the dominant  $^1S_0$  Fock state and two singlet operators with dimension 6 and 8:

$$\mathcal{O}({}^1S_0^{[1]}) = \psi^\dagger \chi \chi^\dagger \psi, \quad (8a)$$

$$\mathcal{P}({}^1S_0^{[1]}) = \frac{1}{2} \left[ \psi^\dagger \chi \chi^\dagger \left( -\frac{i}{2} \overleftrightarrow{\mathbf{D}} \right)^2 \psi + \text{H.c.} \right], \quad (8b)$$

for light hadron decay, and

$$\mathcal{O}_{\text{EM}}({}^1S_0^{[1]}) = \psi^\dagger \chi |0\rangle\langle 0| \chi^\dagger \psi, \quad (9a)$$

$$\mathcal{P}_{\text{EM}}({}^1S_0^{[1]}) = \frac{1}{2} \left[ \psi^\dagger \chi |0\rangle\langle 0| \chi^\dagger \left( -\frac{i}{2} \overleftrightarrow{\mathbf{D}} \right)^2 \psi + \text{H.c.} \right], \quad (9b)$$

for electromagnetic decay. For a generic color-singlet operator of the form  $\mathcal{O}_n = \psi^\dagger \mathcal{K}'_n \chi \chi^\dagger \mathcal{K}_n \psi$ , applying the vacuum-saturation approximation [2], we get

$$\begin{aligned} \langle H | \mathcal{O}_n | H \rangle = & \sum_X \langle H | \psi^\dagger \mathcal{K}'_n \chi | X \rangle \langle X | \chi^\dagger \mathcal{K}_n \psi | H \rangle \\ \approx & \langle H | \psi^\dagger \mathcal{K}'_n \chi | 0 \rangle \langle 0 | \chi^\dagger \mathcal{K}_n \psi | H \rangle, \end{aligned} \quad (10)$$

where the omitted terms are of relative order  $v^4$  and are irrelevant of our calculations here. Therefore, in the following we use the notations

$$\begin{aligned} \langle \mathcal{O}({}^1S_0^{[1]}) \rangle_H := & \langle H({}^1S_0^{[1]}) | \mathcal{O}({}^1S_0^{[1]}) | H({}^1S_0^{[1]}) \rangle \\ \approx & \langle H({}^1S_0^{[1]}) | \mathcal{O}_{\text{EM}}({}^1S_0^{[1]}) | H({}^1S_0^{[1]}) \rangle, \end{aligned} \quad (11a)$$

$$\begin{aligned} \langle \mathcal{P}({}^1S_0^{[1]}) \rangle_H := & \langle H({}^1S_0^{[1]}) | \mathcal{P}({}^1S_0^{[1]}) | H({}^1S_0^{[1]}) \rangle \\ \approx & \langle H({}^1S_0^{[1]}) | \mathcal{P}_{\text{EM}}({}^1S_0^{[1]}) | H({}^1S_0^{[1]}) \rangle. \end{aligned} \quad (11b)$$

Then the decay width of  $^1S_0$  heavy quarkonium at order  $v^2$  is

$$\Gamma(H(^1S_0^{[1]}) \rightarrow \text{LH}) = \frac{F(^1S_0^{[1]})}{m_Q^2} \langle \mathcal{O}(^1S_0^{[1]}) \rangle_H + \frac{G(^1S_0^{[1]})}{m_Q^4} \langle \mathcal{P}(^1S_0^{[1]}) \rangle_H, \quad (12a)$$

$$\Gamma(H(^1S_0^{[1]}) \rightarrow \gamma\gamma) = \frac{F_{\gamma\gamma}(^1S_0^{[1]})}{m_Q^2} \langle \mathcal{O}(^1S_0^{[1]}) \rangle_H + \frac{G_{\gamma\gamma}(^1S_0^{[1]})}{m_Q^4} \langle \mathcal{P}(^1S_0^{[1]}) \rangle_H, \quad (12b)$$

where the leading order LDME is related to the wave function at the origin as

$$\langle \mathcal{O}(^1S_0^{[1]}) \rangle_H = \frac{N_c}{2\pi} |\mathcal{R}_H(0)|^2, \quad (13)$$

and a definition of the ratio of LDMEs is important in this work [20]

$$\langle \mathbf{q}^{2r} \rangle_H = \frac{\langle 0 | \chi^\dagger (-\frac{i}{2} \vec{D})^{2r} \psi | H \rangle}{\langle 0 | \chi^\dagger \psi | H \rangle}, \quad (14)$$

where  $\mathbf{q}$  is half the relative momentum of the heavy quark and antiquark and it is also convenient to define

$$\langle \mathbf{v}^{2r} \rangle_H = \langle \mathbf{q}^{2r} \rangle_H / m_Q^{2r}. \quad (15)$$

To calculate the short-distance coefficients  $F$  and  $G$  in Eq. (12), we use the matching method [2]. Since the short-distance coefficients are insensitive to the long-distance dynamics, we can substitute the bound state with a pair of on shell quark and antiquark separated by a small relative momentum and exploit the equivalence of perturbative QCD and perturbative NRQCD to determine the short-distance coefficients

$$\mathcal{A}(Q\bar{Q} \rightarrow Q\bar{Q})|_{\text{pert QCD}} = \sum_n \frac{f_n(\mu_\Lambda)}{m_Q^{d_n-4}} \langle Q\bar{Q} | \mathcal{O}_n(\mu_\Lambda) | Q\bar{Q} \rangle|_{\text{pert NRQCD}}. \quad (16)$$

The left side of this matching equation can be calculated perturbatively in QCD, and the right side can be calculated perturbatively in NRQCD. Then, we can get the short-distance coefficients  $f_n(\mu_\Lambda)$ , whose imaginary part gives  $F$  and  $G$  in Eq. (12).

### III. KINEMATICS AND METHOD OF CALCULATION

We work in the rest frame of the heavy quarkonium and assume the following notations for the momenta of heavy quark and antiquark

$$p_Q = \frac{1}{2}P + q, \quad (17a)$$

$$p_{\bar{Q}} = \frac{1}{2}P - q, \quad (17b)$$

where

$$P = (2E_q, \mathbf{0}), \quad (18a)$$

$$q = (0, \mathbf{q}), \quad (18b)$$

and  $E_q = \sqrt{m_Q^2 + \mathbf{q}^2}$ .

In our calculation, we adopt the covariant spin-projector method [25–27] to project out the spin-singlet amplitudes. The projector we use is [27]

$$\Pi^0 = \frac{1}{2\sqrt{2}(E_q + m_Q)} \left( \frac{P}{2} + \not{q} + m_Q \right) \times \frac{[(P + 2E_q)\gamma^5(-P + 2E_q)]}{8E_q^2} \left( \frac{P}{2} - \not{q} - m_Q \right). \quad (19)$$

To expand the decay width in terms of  $\mathbf{q}$ , we make the following rescaling for any momentum  $k$ ;

$$k \rightarrow k' E_q / m_Q, \quad (20)$$

which leads all momenta independent of  $\mathbf{q}$ , that is,  $\partial k'_i \cdot k'_j / \partial \mathbf{q} = 0$ . Thus we can expand the amplitudes in  $\mathbf{q}$  before loop integration and phase space integration and extract the S-wave contribution by making the replacement

$$q_\mu q_\nu \rightarrow \frac{\mathbf{q}^2}{D-1} \left[ -g_{\mu\nu} + \frac{P'_\mu P'_\nu}{4m_Q^2} \right], \quad (21)$$

where  $P'_\mu$  is the rescaled momentum of the heavy quarkonium which equals  $(2m_Q, \mathbf{0})$  in its rest frame. Contributions coming from potential regions in perturbative QCD and perturbative NRQCD cancel each other exactly so we neglect these terms to simplify calculations.

### IV. PERTURBATIVE QCD RESULTS

We use FEYNARTS [28,29] to generate Feynman diagrams and amplitudes and use self-written MATHEMATICA codes to perform the remained calculations. Ultraviolet and infrared divergences are regularized with dimensional regularization and  $D = 4 - 2\epsilon$  is assumed. Ultraviolet divergences are removed by renormalization. We define the renormalized heavy quark mass  $m_Q$ , heavy quark field  $\psi_Q$ , and gluon field  $A_\mu$  in the on-mass-shell scheme (OS) and define the QCD coupling constant  $g$  in the  $\overline{\text{MS}}$  scheme, that is,

$$g^0 = Z_g^{\overline{\text{MS}}} g, \quad m_Q^0 = Z_{m_Q}^{\text{OS}} m_Q, \quad (22)$$

$$\psi_Q^0 = \sqrt{Z_2^{\text{OS}}} \psi_Q, \quad A_\mu^0 = \sqrt{Z_3^{\text{OS}}} A_\mu,$$

where terms with superscript 0 denote bare quantities and  $Z_i = 1 + \delta Z_i$  with  $\delta Z_i$  given by

$$\delta Z_{m_Q}^{\text{OS}} = -3C_F \frac{\alpha_s}{4\pi} f_\epsilon \left[ \frac{1}{\epsilon_{\text{UV}}} + \frac{4}{3} + 2\ln(2) \right], \quad (23a)$$

$$\delta Z_2^{\text{OS}} = -C_F \frac{\alpha_s}{4\pi} f_\epsilon \left[ \frac{1}{\epsilon_{\text{UV}}} + \frac{2}{\epsilon_{\text{IR}}} + 6\ln(2) + 4 \right], \quad (23b)$$

$$\delta Z_3^{\text{OS}} = \frac{\alpha_s}{4\pi} f_\epsilon (\beta_0(n_f) - 2C_A) \left( \frac{1}{\epsilon_{\text{UV}}} - \frac{1}{\epsilon_{\text{IR}}} \right), \quad (23c)$$

$$\delta Z_g^{\overline{\text{MS}}} = -\frac{\alpha_s}{4\pi} \frac{\beta_0(n_f)}{2} f_\epsilon \left[ \frac{1}{\epsilon_{\text{UV}}} + \ln\left(\frac{m_Q^2}{\mu_r^2}\right) + 2\ln(2) \right], \quad (23d)$$

where  $f_\epsilon = \Gamma(1 + \epsilon) \left[ \frac{4\pi\mu_r^2}{(2m_Q)^2} \right]^\epsilon$ ,  $\beta_0(n_f) = \frac{11}{3}C_A - \frac{4}{3}T_F n_f$ ,  $\mu_r$  is the renormalization scale and  $n_f$  is the number of light quarks.

### A. $^1S_0^{[1]} \rightarrow \text{LH}$

At leading order in  $\alpha_s$ , there are two diagrams as shown in Fig. 1. The corresponding Born level decay width and its relativistic corrections are

$$\Gamma_{\text{B}}(^1S_0^{[1]} \rightarrow gg) = \frac{1}{2!} \frac{1}{2(2m_Q)} \Phi_{(2D)}(\alpha_s, 4\pi)^2 \frac{16}{9m_Q} \times (1 - 2\epsilon)(1 - \epsilon) \langle \mathcal{O}(^1S_0^{[1]}) \rangle_{\text{LO}}, \quad (24a)$$

$$\Gamma_{\text{B}}^{\text{R}}(^1S_0^{[1]} \rightarrow gg) = -\frac{4}{3} \frac{\mathbf{q}^2}{m_Q^2} \Gamma_{\text{B}}(^1S_0^{[1]} \rightarrow gg), \quad (24b)$$

where  $\Phi_{(2D)} = \frac{1}{8\pi} \frac{\Gamma(1-\epsilon)}{\Gamma(2-2\epsilon)} \left(\frac{\pi}{m_Q}\right)^\epsilon$  is the two-body phase space for  $\mathbf{q} = 0$  in  $D$  dimension. Our results agree with those in Refs. [6,7,9]. At next-to-leading order in  $\alpha_s$ , there are virtual corrections and real corrections. Figure 2 corresponds to Feynman diagrams of virtual corrections, where only distinct forms of diagrams are shown. Contribution of these virtual corrections reads



FIG. 1. Feynman diagrams for  $^1S_0^{[1]} \rightarrow gg$  at Born level.

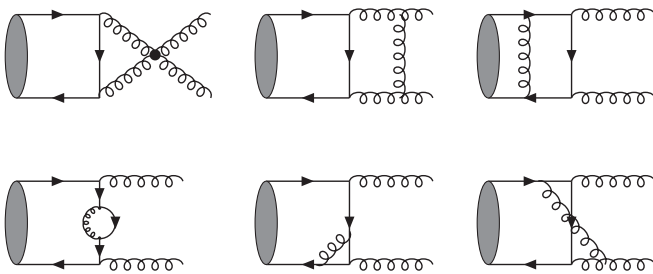


FIG. 2. Representative Feynman diagrams for  $^1S_0^{[1]} \rightarrow gg$  at one-loop level.

$$\begin{aligned} & \Gamma_{\text{V}}(^1S_0^{[1]} \rightarrow gg) \\ &= \frac{C_A \alpha_s}{\pi} \Gamma_{\text{B}}(^1S_0^{[1]} \rightarrow gg) f_\epsilon \left\{ \left[ -\frac{1}{\epsilon^2} + \left( -\frac{11}{6} + \frac{n_f}{9} \right) \frac{1}{\epsilon} \right. \right. \\ &+ \frac{1}{36} \left( -44 + 19\pi^2 + (4n_f - 66) \ln\left(\frac{4m_Q^2}{\mu_r^2}\right) \right) \\ &+ \frac{\mathbf{q}^2}{m_Q^2} \left[ \frac{4}{3} \frac{1}{\epsilon^2} - \frac{4}{27\epsilon} (n_f - 31) + \frac{44}{9} \ln(2) \right. \\ &+ \frac{1}{324} (-4(11 + 24\ln(2))n_f + 24(33 - 2n_f) \\ &\left. \left. \times \ln\left(\frac{m_Q^2}{\mu_r^2}\right) - 267\pi^2 + 874 \right) \right] \right\}. \quad (25) \end{aligned}$$

While other terms agree with those in Refs. [7,9], the result of relativistic correction here is new. Feynman diagrams for real corrections are drawn in Fig. 3 and 4, which correspond to final states with three gluons and  $q\bar{q}g$ , respectively. Results for these two sets of real corrections are

$$\begin{aligned} \Gamma(^1S_0^{[1]} \rightarrow ggg) &= \frac{C_A \alpha_s}{\pi} f_\epsilon \Gamma_{\text{B}}(^1S_0^{[1]} \rightarrow gg) \left\{ \frac{1}{\epsilon^2} + \frac{11}{6\epsilon} + \frac{181}{18} \right. \\ &- \frac{23}{24} \pi^2 + \frac{\mathbf{q}^2}{m_Q^2} \left[ -\frac{4}{3\epsilon^2} - \frac{4}{\epsilon} + \frac{7}{54} \right. \\ &\left. \left. \times (-139 + 12\pi^2) \right] \right\}, \quad (26a) \end{aligned}$$

$$\begin{aligned} \Gamma(^1S_0^{[1]} \rightarrow q\bar{q}g) &= n_f \Gamma_{\text{B}}(^1S_0^{[1]} \rightarrow gg) \frac{\alpha_s}{\pi} \frac{f_\epsilon}{\Gamma(1+\epsilon)\Gamma(1-\epsilon)} \\ &\times T_F \left( -\frac{2}{3\epsilon} - \frac{16}{9} + \frac{\mathbf{q}^2}{m_Q^2} \left( \frac{8}{9\epsilon} + \frac{104}{27} \right) \right). \quad (26b) \end{aligned}$$

While other terms agree with those in Refs. [7,9], the results of relativistic corrections here are new. Adding Eqs. (25) and (26), we obtain the NLO QCD corrections plus relativistic corrections for the light hadron decay width of  $^1S_0$  heavy quarkonium

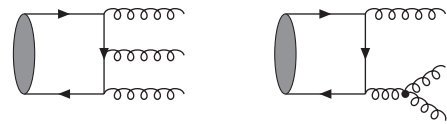


FIG. 3. Representative Feynman diagrams for  $^1S_0^{[1]} \rightarrow ggg$ .

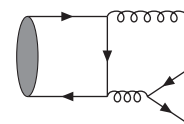


FIG. 4. Representative Feynman diagrams for  $^1S_0^{[1]} \rightarrow q\bar{q}g$ .

$$\begin{aligned} & \Gamma_{\text{QCD}}^{\text{NLO}}(^1S_0^{[1]} \rightarrow \text{LH}) \\ &= \frac{C_A \alpha_s}{\pi} f_\epsilon \Gamma_{\text{B}}(^1S_0^{[1]} \rightarrow gg) \left\{ \frac{1}{216} \left[ -64n_f \right. \right. \\ & \quad \left. \left. + 12(2n_f - 33) \ln\left(\frac{4m_Q^2}{\mu_r^2}\right) - 93\pi^2 + 1908 \right] \right. \\ & \quad \left. + \frac{\mathbf{q}^2}{m_Q^2} \left[ \frac{16}{27\epsilon} + \frac{1}{324} \left( 24 \left( \ln\left(\frac{m_Q^2}{\mu_r^2}\right) + 2 \ln(2) \right) (33 - 2n_f) \right. \right. \right. \\ & \quad \left. \left. \left. + 164n_f + 237\pi^2 - 4964 \right) \right] \right\}. \quad (27) \end{aligned}$$

Adding these terms together, we get the  $^1S_0$  decay width into light hadrons in perturbative QCD

$$\begin{aligned} \Gamma_{\text{QCD}}(^1S_0^{[1]} \rightarrow \text{LH}) &= \Gamma_{\text{B}}(^1S_0^{[1]} \rightarrow gg) \\ & \quad + \Gamma_{\text{B}}^{\text{R}}(^1S_0^{[1]} \rightarrow gg) + \Gamma_{\text{QCD}}^{\text{NLO}}(^1S_0^{[1]} \rightarrow \text{LH}). \quad (28) \end{aligned}$$

### B. $^1S_0^{[1]} \rightarrow \gamma\gamma$

For QCD corrections to the electromagnetic decay, there is no real correction. Diagrams at Born level and one-loop level are the same as those in Fig. 1 and 2 except that the final state gluons are substituted with photons and diagrams containing three-gluon or four-gluon vertexes are excluded. We then get the results

$$\begin{aligned} \Gamma_{\text{B}}(^1S_0^{[1]} \rightarrow \gamma\gamma) &= \frac{1}{2!} \frac{1}{2(2m_Q)} \Phi_{(2D)}(\alpha 4\pi)^2 \frac{8e_Q^4}{m_Q} \\ & \quad \times \langle \mathcal{O}(^1S_0^{[1]}) \rangle_{\text{LO}}, \quad (29a) \end{aligned}$$

$$\Gamma_{\text{B}}^{\text{R}}(^1S_0^{[1]} \rightarrow \gamma\gamma) = -\frac{4}{3} \frac{\mathbf{q}^2}{m_Q^2} \Gamma_{\text{B}}(^1S_0^{[1]} \rightarrow \gamma\gamma), \quad (29b)$$

$$\begin{aligned} \Gamma_{\text{V}}(^1S_0^{[1]} \rightarrow \gamma\gamma) &= \Gamma_{\text{B}}(^1S_0^{[1]} \rightarrow \gamma\gamma) f_\epsilon \frac{\alpha_s}{\pi} \left[ \frac{\pi^2 - 20}{3} \right. \\ & \quad \left. + \frac{\mathbf{q}^2}{m_Q^2} \left( \frac{16}{9\epsilon} + \frac{196 - 15\pi^2}{27} \right) \right], \quad (29c) \end{aligned}$$

where  $e_Q$  is the electric charge of the heavy quark. Results of relativistic corrections in Eq. (29c) are new and the other results agree with those previously calculated as summarized in Ref. [6]. Adding Eqs. (29a)–(29c), we get the result for the  $\gamma\gamma$  decay width of  $^1S_0$  heavy quarkonium in perturbative QCD

$$\begin{aligned} \Gamma_{\text{QCD}}(^1S_0^{[1]} \rightarrow \gamma\gamma) &= \Gamma_{\text{B}}(^1S_0^{[1]} \rightarrow \gamma\gamma) + \Gamma_{\text{B}}^{\text{R}}(^1S_0^{[1]} \rightarrow \gamma\gamma) \\ & \quad + \Gamma_{\text{V}}(^1S_0^{[1]} \rightarrow \gamma\gamma). \quad (30) \end{aligned}$$

## V. PERTURBATIVE NRQCD RESULTS

Order  $\alpha_s v^2$  corrections to the leading order LDME  $\langle \mathcal{O}^0(^1S_0^{[1]}) \rangle$  in perturbative NRQCD have been calculated in Ref. [2], where a cutoff was introduced to regularize the ultraviolet divergences. We rewrite it in dimensional regularization,

$$\begin{aligned} \langle \mathcal{O}^0(^1S_0^{[1]}) \rangle_{\text{NLO}} &= \langle \mathcal{O}^0(^1S_0^{[1]}) \rangle_{\text{LO}} \\ & \quad \times \left[ 1 - \frac{4\alpha_s C_F}{3\pi} \left( \frac{\mu_r^2}{\mu_\Lambda^2} \right)^\epsilon \left( \frac{1}{\epsilon_{\text{UV}}} - \frac{1}{\epsilon_{\text{IR}}} \right) \frac{\mathbf{q}^2}{m_Q^2} \right]. \quad (31) \end{aligned}$$

We define the renormalized operator  $\mathcal{O}^{\text{R}}(^1S_0^{[1]})$  using the  $\overline{\text{MS}}$  scheme

$$\mathcal{O}^0(^1S_0^{[1]}) = Z_{\mathcal{O}}^{\overline{\text{MS}}} \mathcal{O}^{\text{R}}(^1S_0^{[1]}), \quad (32)$$

where

$$Z_{\mathcal{O}}^{\overline{\text{MS}}} = 1 - \frac{4\alpha_s C_F}{3\pi} \left( \frac{\mu_r^2}{\mu_\Lambda^2} \right)^\epsilon \left( \frac{1}{\epsilon_{\text{UV}}} + \ln 4\pi - \gamma_E \right) \frac{\mathbf{q}^2}{m_Q^2}. \quad (33)$$

Therefore

$$\begin{aligned} \langle \mathcal{O}^{\text{R}}(^1S_0^{[1]}) \rangle_{\text{NLO}} &= \left[ 1 + \frac{4\alpha_s C_F}{3\pi} \left( \frac{\mu_r^2}{\mu_\Lambda^2} \right)^\epsilon \left( \frac{1}{\epsilon} + \ln 4\pi - \gamma_E \right) \right. \\ & \quad \left. \times \frac{\mathbf{q}^2}{m_Q^2} \right] \langle \mathcal{O}(^1S_0^{[1]}) \rangle_{\text{LO}}. \quad (34) \end{aligned}$$

Considering that

$$\langle \mathcal{P}(^1S_0^{[1]}) \rangle_{\text{LO}} = \mathbf{q}^2 \langle \mathcal{O}(^1S_0^{[1]}) \rangle_{\text{LO}}, \quad (35)$$

the decay width into light hadrons in perturbative NRQCD becomes

$$\begin{aligned} \Gamma_{\text{NRQCD}}(^1S_0^{[1]} \rightarrow \text{LH}) &= \left\{ F(^1S_0^{[1]}) + \frac{\mathbf{q}^2}{m_Q^2} \left[ G(^1S_0^{[1]}) + \frac{4\alpha_s C_F}{3\pi} \left( \frac{\mu_r^2}{\mu_\Lambda^2} \right)^\epsilon \right. \right. \\ & \quad \left. \left. \times \left( \frac{1}{\epsilon} + \ln 4\pi - \gamma_E \right) F(^1S_0^{[1]}) \right] \right\} \frac{\langle \mathcal{O}(^1S_0^{[1]}) \rangle_{\text{LO}}}{m_Q^2}. \quad (36) \end{aligned}$$

The electromagnetic decay rate can be obtained by replacing  $F(^1S_0^{[1]})$  and  $G(^1S_0^{[1]})$  with  $F_{\gamma\gamma}(^1S_0^{[1]})$  and  $G_{\gamma\gamma}(^1S_0^{[1]})$ , respectively.

## VI. MATCHING

Finally we obtain the short-distance coefficients by equating results from perturbative QCD in Eqs. (28) and (30) with that from perturbative NRQCD in Eq. (36)



$$F(^1S_0^{[1]}) = \frac{4\pi\alpha_s^2}{9} \left[ 1 + \frac{\alpha_s}{\pi} \frac{-64n_f + 12(2n_f - 33) \ln\left(\frac{4m_Q^2}{\mu_r^2}\right) - 93\pi^2 + 1908}{72} \right], \quad (37a)$$

$$G(^1S_0^{[1]}) = \frac{4\pi\alpha_s^2}{9} \left\{ -\frac{4}{3} + \frac{\alpha_s}{\pi} \frac{1}{108} [48 \ln(2)(25 - 2n_f) + 164n_f - 4964 + 24(33 - 2n_f) \ln\left(\frac{m_Q^2}{\mu_r^2}\right) + 192 \ln\left(\frac{\mu_\Lambda^2}{m_Q^2}\right) + 237\pi^2] \right\}, \quad (37b)$$

$$F_{\gamma\gamma}(^1S_0^{[1]}) = 2\pi\alpha^2 e_Q^4 \left( 1 + \frac{\alpha_s}{\pi} \frac{\pi^2 - 20}{3} \right), \quad (37c)$$

$$G_{\gamma\gamma}(^1S_0^{[1]}) = 2\pi\alpha^2 e_Q^4 \left\{ -\frac{4}{3} + \frac{\alpha_s}{\pi} \frac{1}{27} \left[ 48 \ln\left(\frac{\mu_\Lambda^2}{m_Q^2}\right) - 96 \ln(2) - 15\pi^2 + 196 \right] \right\}, \quad (37d)$$

where QCD corrections for  $G(^1S_0^{[1]})$  and  $G_{\gamma\gamma}(^1S_0^{[1]})$  are new while the other results agree with those in Refs. [2,6,7,9]. With these short-distance coefficients, we can update the decay widths of  $^1S_0$  heavy quarkonium into light hadrons and two photons.

## VII. PHENOMENOLOGY

The above obtained result can be used in  $^1S_0$  charmonium and bottomonium decays. In the following we will focus on the  $\eta_c$  decay width into light hadrons (approximately the total width) and decay width into two photons. In these decays there are two unknown LDMEs. In principle, one can fix these LDMEs either through direct fit with experimental data [30] or calculation from lattice QCD [17,18]. The order  $v^2$  LDME is ultraviolet divergent and needs to be regularized [20]. For lattice calculations this is performed by imposing a hard cutoff regulator. However, due to slow convergence of this regularization, the results available from lattice calculations of order  $v^2$  LDME suffer from large uncertainties [17,18]. On the other hand, we find that direct fit of the two LDMEs using experimental measurements of  $\gamma\gamma$  width and total width of  $\eta_c$  can not give reliable values due to the approximate linear dependence of the two theoretical predictions for these two decays.

Therefore, we determine the two LDMEs using the potential model method recently introduced in Refs. [19–21]. A widely accepted potential model, the Cornell potential [31]

$$V(r) = -\frac{\kappa}{r} + \sigma r, \quad (38)$$

is chosen in this work. Since the spin dependent effect is not included in this potential, the LDMEs calculated this way are accurate up to corrections of relative order  $v^2$ . However, as argued in Ref. [20], this error is in fact much less than the order  $v^2$  (about 30%), thus we attach an uncertainty of 30% to the central value of the order  $v^2$  LDMEs to account for the error due to this static potential approximation.

In solving the Schrödinger equation [32], there are three unknown parameters.  $\sigma = 0.1682 \pm 0.0053 \text{ GeV}^2$  is taken from the average of lattice calculations [20] and the mass parameter is expressed in terms of the  $1S$ - $2S$  mass splitting [19,20]. Here we take  $m(\psi(2S)) - m(J/\psi) = 589.188 \pm 0.028 \text{ MeV}$  [33]. The last remaining parameter is fixed by equating theoretical predictions to experimentally measured results. When we use the decay width formula, we resum a class of relativistic corrections at leading order in  $\alpha_s$  for  $\gamma\gamma$  decay as in Refs. [20,21]. For the experimental input, we make use of this approximation  $\Gamma^{\text{LH}}(\eta_c(nS)) = \Gamma^{\text{total}}(\eta_c(nS))$ . For  $\eta_c$ , we use  $\Gamma^{\gamma\gamma}(\eta_c)$  (or  $\Gamma^{\text{LH}}(\eta_c)$ ) as input to obtain one set LDMEs, which are then utilized to obtain  $\Gamma^{\text{LH}}(\eta_c)$  (or  $\Gamma^{\gamma\gamma}(\eta_c)$ ). For  $\eta_c(2S)$ , we use the total width as input and make predictions for the  $\gamma\gamma$  decay width. We take  $m_c$  to be  $1.4 \pm 0.2 \text{ GeV}$  [20],  $\alpha = 1/137$ ,  $\Lambda_{\text{QCD}} = 0.39 \text{ GeV}$  and vary the renormalization scale  $\mu_r$  and NRQCD factorization scale  $\mu_\Lambda$  separately from 1 GeV to 3 GeV with 2 GeV

TABLE I. LDMEs obtained from potential model for  $\eta_c$  and the predicted total width of  $\eta_c$ , the superscript  $\gamma\gamma$  indicates that the observed width of  $\eta_c \rightarrow \gamma\gamma$  is used as input. The second row gives central values while the followed rows give variations with respect to related parameters.

Case	$ \mathcal{R}_{\eta_c}^{\gamma\gamma}(0) ^2(\text{GeV}^3)$	$\langle \mathbf{v}^2 \rangle_{\eta_c}^{\gamma\gamma}$	$\Gamma^{\text{total}}(\eta_c)$ (MeV)
Central	0.881	0.228	31.4
$+\Delta\langle \mathbf{v}^2 \rangle_{\eta_c}$	0.078	0.068	-3.5
$-\Delta\langle \mathbf{v}^2 \rangle_{\eta_c}$	-0.075	-0.068	2.6
$+\Delta m_c$	0.187	-0.065	0.3
$-\Delta m_c$	-0.167	0.102	-3.4
$+\Delta\sigma$	0.022	0.020	-0.9
$-\Delta\sigma$	-0.021	-0.019	0.8
$+\Delta\mu_r$	-0.059	0.005	-9.2
$-\Delta\mu_r$	0.217	-0.018	27.3
$+\Delta\mu_\Lambda$	-0.036	0.003	-0.6
$-\Delta\mu_\Lambda$	0.064	-0.005	1.1
$+\Delta\Gamma_{\eta_c}$	0.232	-0.019	10.3
$-\Delta\Gamma_{\eta_c}$	-0.243	0.021	-9.9

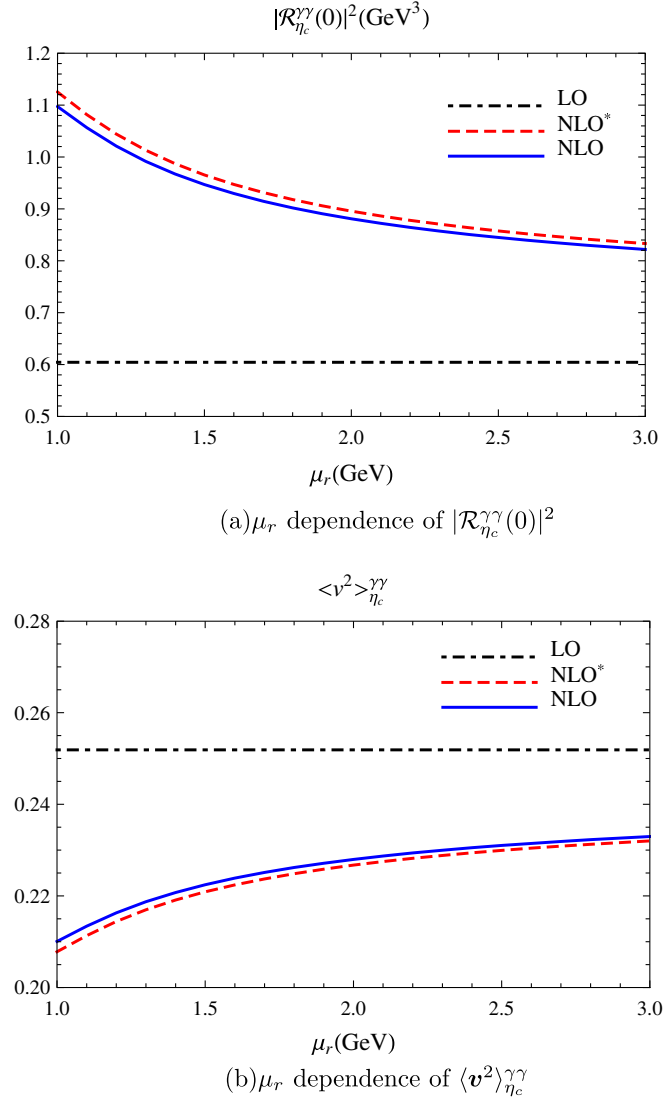


FIG. 5 (color online).  $\mu_r$  dependence of LDMEs for  $\eta_c$  using the observed  $\gamma\gamma$  width as input. LO represents values without QCD corrections, NLO\* includes QCD corrections only for terms at leading order in  $v$ , and NLO takes into account our new QCD corrections to order  $v^2$  terms.

as the central value. The LDMEs are expressed in terms of the wave function at the origin  $|\mathcal{R}(0)|^2$  and  $\langle v^2 \rangle$  as defined in Eqs. (13) and (15). In each determination of these LDMEs and the corresponding decay width, we evaluate the variations caused by the uncertainties of the parameters and summarize them in the tables. Because the potential does not take into account of the spin effects, we attach each  $v^2$  LDME an uncertainty  $\langle v^2 \rangle$  of 30% of the central value. In each case, various uncertainties are added in quadrature to give the total uncertainty.

For  $\eta_c$ , with the  $\gamma\gamma$  width  $\Gamma^{\gamma\gamma}(\eta_c) = 7.2 \pm 0.7 \pm 2.0$  KeV [33] as input, the determined LDMEs are

$$|\mathcal{R}_{\eta_c}^{\gamma\gamma}(0)|^2 = 0.881^{+0.382}_{-0.313} \text{ GeV}^3, \quad (39a)$$

$$\langle v^2 \rangle_{\eta_c}^{\gamma\gamma} = 0.228^{+0.126}_{-0.100}, \quad (39b)$$

where the superscript  $\gamma\gamma$  indicates that we use the  $\gamma\gamma$  decay width as input. Various uncertainties are summarized in Table I. The most significant uncertainty comes from the experimental data. At order  $\alpha_s v^2$ , another dependence on NRQCD factorization scale  $\mu_\Lambda$  is introduced. However, as we can see from Table I, variations of LDMEs are small when we change  $\mu_\Lambda$  from 1 GeV to 3 GeV. In Fig. 5, we present  $\mu_r$  dependence of three sets of LDMEs in terms of  $|\mathcal{R}_{\eta_c}(0)|^2$  and  $\langle v^2 \rangle_{\eta_c}$ , where the other parameters are fixed to their central values. Of these three sets of lines, LO represents calculation without any QCD corrections, NLO\* corresponds to that including QCD corrections but only for terms at leading order in  $v$ , and NLO means our new result with order  $\alpha_s v^2$  correction taken into account. The LDMEs corresponding to NLO\* have been computed earlier in Ref. [20] and can be compared here with the values including the new order  $\alpha_s v^2$  corrections. We can see from this figure that these two lines are close to each other, which reflects the fact that the effect of the new order  $\alpha_s v^2$  correction is not large. Utilizing this set of LDMEs as input, we get the total decay width for  $\eta_c$

$$\Gamma^{\text{total}}(\eta_c) = 31.4^{+29.3}_{-14.4} \text{ MeV}. \quad (40)$$

This value is in consistency with experimental measurement  $28.6 \pm 2.2$  MeV [33], although there are large uncertainties. The details of the uncertainties are summarized in Table I. Here, the uncertainty induced by the  $\mu_r$  dependence predominates over that from the experimental input of the  $\gamma\gamma$  width of  $\eta_c$ .

If, on the other hand, we use the total width of  $\eta_c$ ,  $\Gamma^{\text{total}}(\eta_c) = 28.6 \pm 2.2$  MeV [33] as input, then we get another set of LDMEs

TABLE II. LDMEs obtained from potential model for  $\eta_c$  and the predicted  $\gamma\gamma$  width of  $\eta_c$ , where the superscript LH indicates that the observed total width of  $\eta_c$  is used as input. The second row gives the central values while the followed rows give variations with respect to related parameters.

Case	$ \mathcal{R}_{\eta_c}^{\text{LH}}(0) ^2$ (GeV <sup>3</sup> )	$\langle v^2 \rangle_{\eta_c}^{\text{LH}}$	$\Gamma(\eta_c \rightarrow \gamma\gamma)$ (KeV)
Central	0.814	0.234	6.61
$+\Delta\langle v^2 \rangle_{\eta_c}$	0.194	0.070	0.90
$-\Delta\langle v^2 \rangle_{\eta_c}$	-0.131	-0.070	-0.54
$+\Delta m_c$	0.163	-0.065	-0.07
$-\Delta m_c$	-0.090	0.095	0.71
$+\Delta\sigma$	0.042	0.018	0.19
$-\Delta\sigma$	-0.038	-0.018	-0.16
$+\Delta\mu_r$	0.201	-0.017	2.47
$-\Delta\mu_r$	-0.189	0.016	-2.73
$+\Delta\mu_\Lambda$	-0.020	0.002	0.13
$-\Delta\mu_\Lambda$	0.036	-0.003	-0.21
$+\Delta\Gamma_{\eta_c}$	0.052	-0.004	0.46
$-\Delta\Gamma_{\eta_c}$	-0.053	0.005	-0.47

$$|\mathcal{R}_{\eta_c}^{\text{LH}}(0)|^2 = 0.814_{-0.256}^{+0.332} \text{ GeV}^3, \quad (41a)$$

$$\langle \mathbf{v}^2 \rangle_{\eta_c}^{\text{LH}} = 0.234_{-0.099}^{+0.121}, \quad (41b)$$

where the superscript LH indicates that we use the total width of  $\eta_c$  as input. Variations with respect to the parameters are summarized in Table II. The experimental uncertainty in this case is small and the main uncertainty comes from the relatively strong  $\mu_r$  dependence of the theoretical prediction. The  $\mu_r$  dependence of the two LDMEs is shown in Fig. 6. As in previous case, we display another two sets of LDMEs, where only QCD corrections at leading order in  $v$  are taken into account or no QCD correction is considered. The two sets with QCD corrections show great improvement of  $\mu_r$  dependence with

respect to the one without QCD corrections, and they are almost parallel to each other. The only difference between the two sets of values is that the  $\alpha_s v^2$  correction enhances  $|\mathcal{R}_{\eta_c}(0)|^2$  by about 30%. This enhanced LDME coincides with previously obtained value using  $\Gamma^{\gamma\gamma}(\eta_c)$  as input. The value of  $\langle \mathbf{v}^2 \rangle_{\eta_c}$  is relatively stable. With this set of LDMEs, we obtain the  $\gamma\gamma$  decay width

$$\Gamma^{\gamma\gamma}(\eta_c) = 6.61_{-2.83}^{+2.77} \text{ KeV}, \quad (42)$$

which is also consistent with the experimental measurement  $7.2 \pm 0.7 \pm 2.0 \text{ KeV}$  [33].

Since now we have two sets of values for the two LDMEs for  $\eta_c$  in Eqs. (39) and (41), we can combine these values to get a better estimation. The uncertainties in Table I and II are correlated, and we use the method in Ref. [20] to treat these correlations. First, we construct a two-by-two covariance matrix for  $\langle \mathcal{O}(^1S_0^{[1]}) \rangle_{\eta_c}^{\gamma\gamma}$  and  $\langle \mathcal{O}(^1S_0^{[1]}) \rangle_{\eta_c}^{\text{LH}}$ . It describes correlations between the variations in the two tables and is defined as  $C_{jk} = \sum_i \Delta_{ji} \Delta_{ki}$  with  $\Delta_{ji} = \frac{1}{2}(O_{ji}^+ - O_{ji}^-)$ . The indexes  $j, k$  refer to these two leading order LDMEs and  $i$  runs through every item in Table I and II.  $O_{ji}^+$  and  $O_{ji}^-$  correspond to the plus and minus variations of the LDMEs. For the  $i$ -th item in Table I or Table II, we define the  $\chi_i^2$  as

$$\chi_i^2 = \sum_{j,k} (O_{ji} - \bar{O}_i)(C^{-1})_{jk}(O_{ki} - \bar{O}_i) \quad (43)$$

and minimize it to get the average value  $\bar{O}_i$  for  $\langle \mathcal{O}(^1S_0^{[1]}) \rangle_{\eta_c}$ . Once we obtain the values of  $\langle \mathcal{O}(^1S_0^{[1]}) \rangle_{\eta_c}$ , we use the potential model to get the values of  $\langle \mathcal{P}(^1S_0^{[1]}) \rangle_{\eta_c}$ . We perform this calculation for each of the items in Table I and II, treat the renormalization scale  $\mu_r$  and NRQCD factorization scale  $\mu_\Lambda$  simply as the same quantities in the two tables and express the results in terms of  $|\mathcal{R}_{\eta_c}(0)|$  and  $\langle \mathbf{v}^2 \rangle_{\eta_c}$ . The results are

$$|\mathcal{R}_{\eta_c}(0)|^2 = 0.834_{-0.197}^{+0.281} \text{ GeV}^3, \quad (44a)$$

$$\langle \mathbf{v}^2 \rangle_{\eta_c} = 0.232_{-0.098}^{+0.121}, \quad (44b)$$

with the details of the uncertainties given in Table III. We note that the uncertainties here for  $|\mathcal{R}_{\eta_c}(0)|^2$  are smaller than those in Eqs. (39) and (41).

For  $\eta_c(2S)$ , we use the observed total width  $14 \pm 7 \text{ MeV}$  [33] as input and get the LDMEs for  $\eta_c(2S)$

$$|\mathcal{R}_{\eta_c(2S)}^{\text{LH}}(0)|^2 = 0.423_{-0.230}^{+0.245} \text{ GeV}^3, \quad (45a)$$

$$\langle \mathbf{v}^2 \rangle_{\eta_c(2S)}^{\text{LH}} = 0.255_{-0.109}^{+0.130}. \quad (45b)$$

Some potential model calculations of the squared wave function at the origin in Ref. [34] give 0.418 for the logarithmic potential [35], 0.529 for the QCD-motivated potential model proposed by Buchmüller and Tye[36], and 0.559 for the power-law potential [37]. Our result is consistent with their values. Table IV gives details with various

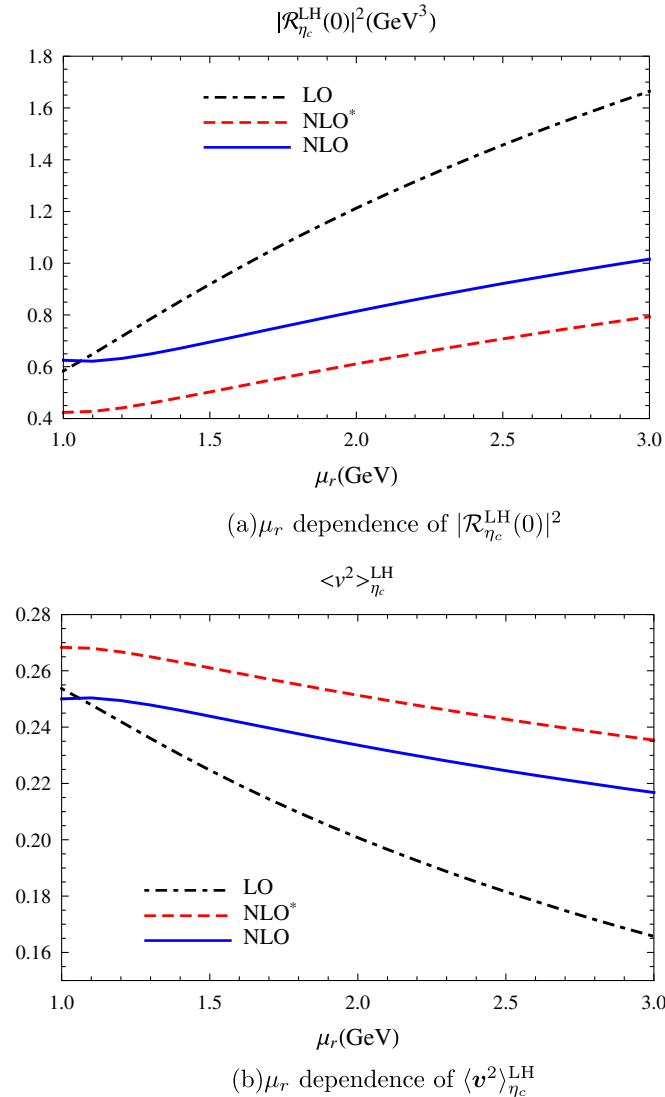


FIG. 6 (color online).  $\mu_r$  dependence of LDMEs for  $\eta_c$  using the observed total width as input. LO represents values without QCD corrections, NLO\* includes QCD corrections only for terms at leading order in  $v$ , and NLO takes into account our new QCD corrections to order  $v^2$  terms.



TABLE III. The averages of the LDMEs for  $\eta_c$ . The second row gives the central values and subsequent rows give variations with respect to various uncertainties.

Case	$ \mathcal{R}_{\eta_c}(0) ^2$ (GeV <sup>3</sup> )	$\langle v^2 \rangle_{\eta_c}$
Central	0.834	0.232
$+\Delta\langle v^2 \rangle_{\eta_c}$	0.159	0.070
$-\Delta\langle v^2 \rangle_{\eta_c}$	-0.115	-0.070
$+\Delta m_c$	0.170	-0.065
$-\Delta m_c$	-0.113	0.097
$+\Delta\sigma$	0.036	0.019
$-\Delta\sigma$	-0.033	-0.018
$+\Delta\mu_r$	0.124	-0.010
$-\Delta\mu_r$	-0.069	0.006
$+\Delta\mu_\Lambda$	-0.025	0.002
$-\Delta\mu_\Lambda$	0.044	-0.004
$+\Delta\Gamma_{\eta_c}^{\gamma\gamma}$	0.069	-0.006
$-\Delta\Gamma_{\eta_c}^{\gamma\gamma}$	-0.072	0.006
$+\Delta\Gamma_{\eta_c}^{\text{total}}$	0.037	-0.003
$-\Delta\Gamma_{\eta_c}^{\text{total}}$	-0.037	0.003

TABLE IV. LDMEs obtained from potential model for  $\eta_c(2S)$  and the predicted  $\gamma\gamma$  width of  $\eta_c(2S)$ , where the superscript LH indicates that the total width of  $\eta_c(2S)$  is used as input. The second row gives the central values while the followed rows give variations with respect to related parameters.

Case	$ \mathcal{R}_{\eta_c}^{\text{LH}}(0) ^2$ (GeV <sup>3</sup> )	$\langle v^2 \rangle_{\eta_c}^{\text{LH}}$	$\Gamma(\eta_c(2S) \rightarrow \gamma\gamma)$ (KeV)
Central	0.423	0.255	3.34
$+\Delta\langle v^2 \rangle_{\eta_c(2S)}$	0.121	0.076	0.58
$-\Delta\langle v^2 \rangle_{\eta_c(2S)}$	-0.077	-0.076	-0.33
$+\Delta m_c$	0.077	-0.069	-0.08
$-\Delta m_c$	-0.035	0.099	0.47
$+\Delta\sigma$	0.024	0.019	0.11
$-\Delta\sigma$	-0.022	-0.019	-0.10
$+\Delta\mu_r$	0.102	-0.016	1.22
$-\Delta\mu_r$	-0.091	0.014	-1.33
$+\Delta\mu_\Lambda$	-0.012	0.002	0.07
$-\Delta\mu_\Lambda$	0.022	-0.003	-0.11
$+\Delta\Gamma_{\eta_c(2S)}$	0.167	-0.026	1.47
$-\Delta\Gamma_{\eta_c(2S)}$	-0.192	0.029	-1.58

uncertainties. In the  $\eta_c(2S)$  case, both the  $\mu_r$  dependence of theoretical result and the experimental input of the total width have large uncertainties and therefore the LDMEs are subject to relatively large uncertainties. In Fig. 7, we present  $\mu_r$  dependence of this set of LDMEs. The shape of the lines is similar to Fig. 6 except the value for  $|\mathcal{R}_{\eta_c(2S)}(0)|^2$  here is smaller by about a factor of 2. Exploiting this set of LDMEs, we can make predictions for the  $\gamma\gamma$  decay width of  $\eta_c(2S)$ ,

$$\Gamma^{\gamma\gamma}(\eta_c(2S)) = 3.34^{+2.06}_{-2.10} \text{ KeV}. \quad (46)$$

This prediction is consistent with the experimental observation that the branching fraction of  $\gamma\gamma$  decay is

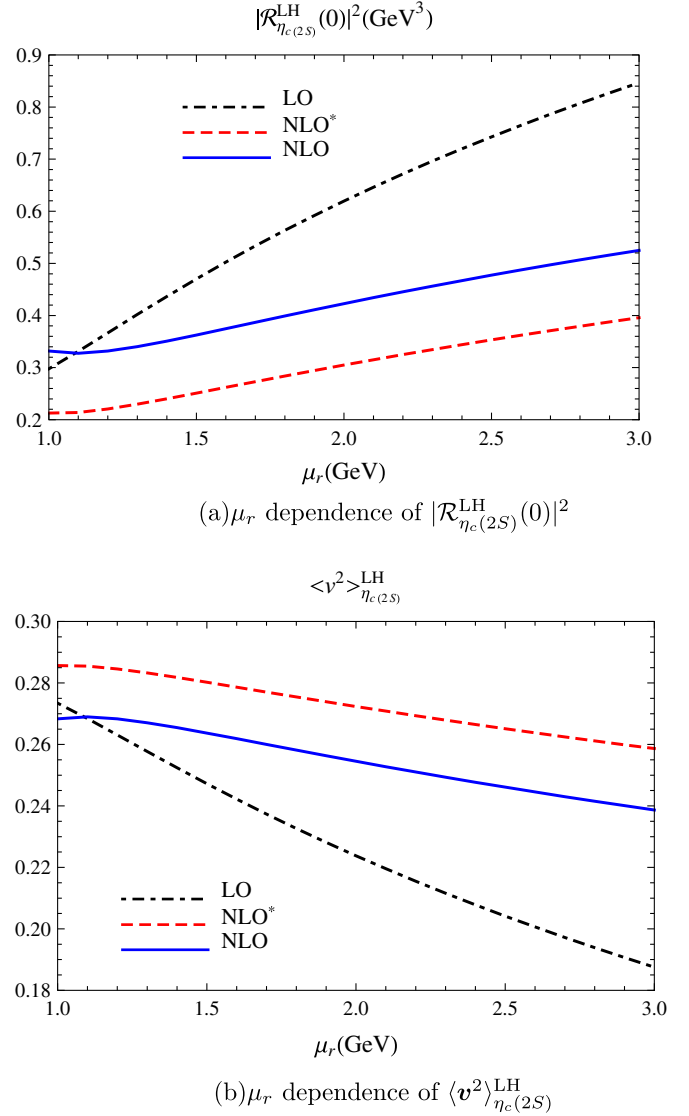


FIG. 7 (color online).  $\mu_r$  dependence of LDMEs for  $\eta_c(2S)$  using the total width as input. LO represents values without QCD corrections, NLO\* includes QCD corrections only for terms at leading order in  $v$ , and NLO takes into account our new QCD corrections to order  $v^2$  terms.

smaller than  $5 \times 10^{-4}$  [33]. Another experiment measured  $\Gamma_{\gamma\gamma}(\eta_c(2S))B(\eta_c(2S) \rightarrow K\bar{K}\pi) = (0.18 \pm 0.05 \pm 0.02)\Gamma_{\gamma\gamma}(\eta_c(1S))B(\eta_c(1S) \rightarrow K\bar{K}\pi)$  [38] and assumed that the branching fractions of  $\eta_c$  and  $\eta_c(2S)$  decays into  $K_S K \pi$  were equal and made use of  $\Gamma(\eta_c \rightarrow \gamma\gamma) = 7.4 \pm 0.4 \pm 2.3 \text{ KeV}$  and then derived  $\Gamma(\eta_c(2S)) = 1.3 \pm 0.6 \text{ KeV}$  [33,38]. Our result is not in contradiction with their measurement within errors.

### VIII. SUMMARY

Within the framework of NRQCD, we calculate order  $\alpha_s v^2$  corrections to decays of  $^1S_0$  heavy quarkonium into light hadrons and two photons. In both processes, infrared

divergences are found to be canceled through the matching of perturbative QCD and perturbative NRQCD results. There are two unknown NRQCD LDMEs, which are determined using potential model method [19–21] either with the observed total width or two photon width as input. When using  $\Gamma^{\gamma\gamma}(\eta_c)$  as input, we get  $|\mathcal{R}_{\eta_c}^{\gamma\gamma}(0)|^2 = 0.881_{-0.313}^{+0.382} \text{ GeV}^3$  and  $\langle v^2 \rangle_{\eta_c}^{\gamma\gamma} = 0.228_{-0.100}^{+0.126}$ , from which we predict  $\Gamma^{\text{total}}(\eta_c) = 31.4_{-14.4}^{+29.3} \text{ MeV}$ . Alternatively, when using  $\Gamma^{\text{total}}(\eta_c)$  as input, we get  $|\mathcal{R}_{\eta_c}^{\text{LH}}(0)|^2 = 0.814_{-0.256}^{+0.332} \text{ GeV}^3$  and  $\langle v^2 \rangle_{\eta_c}^{\text{LH}} = 0.234_{-0.099}^{+0.121}$ , and we predict the  $\gamma\gamma$  width of  $\eta_c$  to be  $\Gamma^{\gamma\gamma}(\eta_c) = 6.61_{-2.83}^{+2.77} \text{ KeV}$ . All these predictions agree well with experimental data. We then combine these two kinds of determination of LDMEs and get the average values  $|\mathcal{R}_{\eta_c}(0)|^2 = 0.834_{-0.197}^{+0.281} \text{ GeV}^3$  and  $\langle v^2 \rangle_{\eta_c} = 0.232_{-0.098}^{+0.121}$ . For  $\eta_c(2S)$ , we use the observed total width as input and find  $|\mathcal{R}_{\eta_c(2S)}^{\text{LH}}(0)|^2 = 0.423_{-0.230}^{+0.245} \text{ GeV}^3$  and  $\langle v^2 \rangle_{\eta_c(2S)} = 0.255_{-0.109}^{+0.130}$ . With this set of LDMEs, we predict the  $\gamma\gamma$  width of  $\eta_c(2S)$  to be  $3.34_{-2.10}^{+2.06} \text{ KeV}$ , which is not in

contradiction with data within uncertainties. Consequently, the order  $\alpha_s v^2$  corrections (especially the one to the decay into light hadrons) are found to have significant effects on improving the consistency between theoretical predictions and experimental measurements.

## ACKNOWLEDGMENTS

We thank G. T. Bodwin, Y. Fan, and C. Meng for helpful discussions. We also thank Franz F. Schöberl for providing us with `schrodinger.nb` to solve the Schrödinger equation. This work was supported by the National Natural Science Foundation of China (Grants No. 11021092, No. 11075002) and the Ministry of Science and Technology of China (Grant No. 2009CB825200).

*Note added.*—When we finished the calculations and are preparing this paper, a related work appears [39] that also gives  $\alpha_s v^2$  corrections to the  $\gamma\gamma$  decay width. We find our results for this channel agree with theirs, while we have also calculated the light hadron decay width.

- 
- [1] W. E. Caswell and G. P. Lepage, *Phys. Lett. B* **167**, 437 (1986).
- [2] G. T. Bodwin, E. Braaten, and G. P. Lepage, *Phys. Rev. D* **51**, 1125 (1995); **55**, 5853(E) (1997).
- [3] R. Barbieri, E. d’Emilio, G. Curci, and E. Remiddi, *Nucl. Phys. B* **154**, 535 (1979).
- [4] K. Hagiwara, C. B. Kim, and T. Yoshino, *Nucl. Phys. B* **177**, 461 (1981).
- [5] I. Harris and L. M. Brown, *Phys. Rev.* **105**, 1656 (1957).
- [6] G. T. Bodwin and A. Petrelli, *Phys. Rev. D* **66**, 094011 (2002).
- [7] A. Petrelli, M. Cacciari, M. Greco, F. Maltoni, and M. L. Mangano, *Nucl. Phys. B* **514**, 245 (1998).
- [8] H.-W. Huang, J.-H. Liu, J. Tang, and K.-T. Chao, *Phys. Rev. D* **56**, 368 (1997).
- [9] Y. Fan, Z.-G. He, Y.-Q. Ma, and K.-T. Chao, *Phys. Rev. D* **80**, 014001 (2009).
- [10] D. Ebert, R. N. Faustov, and V. O. Galkin, *Mod. Phys. Lett. A* **18**, 601 (2003).
- [11] J. P. Lansberg and T. N. Pham, *Phys. Rev. D* **74**, 034001 (2006).
- [12] J. P. Lansberg and T. N. Pham, *Phys. Rev. D* **75**, 017501 (2007).
- [13] A. Czarnecki and K. Melnikov, *Phys. Lett. B* **519**, 212 (2001).
- [14] W.-Y. Keung and I. J. Muzinich, *Phys. Rev. D* **27**, 1518 (1983).
- [15] N. Brambilla, E. Mereghetti, and A. Vairo, *Phys. Rev. D* **79**, 074002 (2009).
- [16] N. Brambilla, E. Mereghetti, and A. Vairo, *J. High Energy Phys.* **08** (2006) 039.
- [17] G. T. Bodwin, D. K. Sinclair, and S. Kim, *Phys. Rev. Lett.* **77**, 2376 (1996).
- [18] G. T. Bodwin, D. K. Sinclair, and S. Kim, *Phys. Rev. D* **65**, 054504 (2002).
- [19] G. T. Bodwin, D. Kang, and J. Lee, *Phys. Rev. D* **74**, 014014 (2006).
- [20] G. T. Bodwin, H. S. Chung, D. Kang, J. Lee, and C. Yu, *Phys. Rev. D* **77**, 094017 (2008).
- [21] H. S. Chung, J. Lee, and C. Yu, *Phys. Lett. B* **697**, 48 (2011).
- [22] N. Brambilla, A. Pineda, J. Soto, and A. Vairo, *Nucl. Phys. B* **566**, 275 (2000).
- [23] A. Pineda and A. Vairo, *Phys. Rev. D* **63**, 054007 (2001).
- [24] S. Fleming, I. Z. Rothstein, and A. K. Leibovich, *Phys. Rev. D* **64**, 036002 (2001).
- [25] J. H. Kuhn, J. Kaplan, and E. G. O. Safiani, *Nucl. Phys. B* **157**, 125 (1979).
- [26] B. Guberina, J. H. Kuhn, R. D. Peccei, and R. Ruckl, *Nucl. Phys. B* **174**, 317 (1980).
- [27] W.-Y. Keung and I. J. Muzinich, *Phys. Rev. D* **27**, 1518 (1983).
- [28] J. Kublbeck, M. Bohm, and A. Denner, *Comput. Phys. Commun.* **60**, 165 (1990).
- [29] T. Hahn, *Comput. Phys. Commun.* **140**, 418 (2001).
- [30] Z.-G. He, Y. Fan, and K.-T. Chao, *Phys. Rev. D* **75**, 074011 (2007).
- [31] E. Eichten, K. Gottfried, T. Kinoshita, K. D. Lane, and T.-M. Yan, *Phys. Rev. D* **17**, 3090 (1978); **21**, 313(E) (1980); **21**, 203 (1980).
- [32] W. Lucha and F. F. Schoberl, *Int. J. Mod. Phys. C* **10**, 607 (1999).
- [33] K. Nakamura *et al.* (Particle Data Group Collaboration), *J. Phys. G* **37**, 075021 (2010).
- [34] E. J. Eichten and C. Quigg, *Phys. Rev. D* **52**, 1726 (1995).

- [35] C. Quigg and J.L. Rosner, *Phys. Lett. B* **71**, 153 (1977).
- [36] W. Buchmüller and S.H.H. Tye, *Phys. Rev. D* **24**, 132 (1981).
- [37] A. Martin, *Phys. Lett. B* **93**, 338 (1980).
- [38] D.M. Asner *et al.* (CLEO Collaboration), *Phys. Rev. Lett.* **92**, 142001 (2004).
- [39] Y. Jia, X.-T. Yang, W.-L. Sang, and J. Xu, arXiv:1104.1418.